

# **A 1D co-simulation approach for the prediction of pollutant emissions of internal combustion engines**

T. Cerri, G. D'Errico, G. Montenegro, A. Onorati  
Politecnico di Milano

G. Koltsakis, Z. Samaras  
Aristotle University of Thessaloniki

V. Tziolas, N. Zingopis, K. Michos  
Exothermia SA

J. Rojewski, V. Papetti, P. Dimopoulos Eggenschwiler and P. Soltic  
EMPA, Swiss Federal Laboratories for Materials Science and Technology

## 1 Abstract

The prediction of pollutant emissions generated by IC engines has been a challenge since the introduction of the emission regulation legislation. This paper describes the approach followed by the authors to strictly couple two different 1D modeling tools in a co-simulation environment, to achieve a reliable calculation of engine-out and tailpipe emissions. The main idea is to allow an accurate 1D simulation of the unsteady flows and wave action inside the intake and exhaust systems, without resorting to over-simplified geometrical discretization, and to rely on advanced combustion models and kinetic sub-models for the calculation of cylinder-out emissions. A specific fluid dynamic approach is then used to track the composition along the exhaust system, in order to evaluate the conversion efficiency of after-treatment devices, such as TWC, GPF, DPF, DOC, SCR and so on. This co-simulation environment is validated against a real engine configuration which was instrumented and tested at EMPA labs. A 4 cylinder SI, turbocharged, CNG engine is investigated at different loads and revolution speeds, to allow a wide validation with experimental data and verify the predictiveness of engine performances and pollutant emissions.

## 2 Introduction

The current European legislation concerning pollutant emissions from IC engine vehicles is very stringent and demanding. In addition, the CO<sub>2</sub> fleet emission must obey to a significant reduction path during the next decade, to cope with the prescribed targets recently agreed.

In general, the prediction of pollutant emissions from IC engines has been a challenge since the introduction of the emission regulation legislation. During the last decade, along with the more tightening limits and increased public concern about air quality, the capability of simulating different operating conditions and driving cycles with acceptable computational effort has become a key feature for modern simulation codes.

Today advanced simulation tools give the opportunity to investigate how to achieve high efficiency, low fuel consumption and emissions while keeping good performances, on the basis of the typical operating conditions of the WLTP cycle and the new Real Driving Emission (RDE) homologation procedure.

The role of 1D thermo-fluid dynamic simulation models is extremely important to achieve this task, in order to investigate the performances of next generation of IC engines working over a large range of operating conditions.

Many 1D simulation tools are available on the market, offering real time models capable of achieving the simulation of any driving cycle in limited time frames. These

approaches are based on the extreme simplification of the engine geometry or on the adoption of engine maps, which, for any engine operating condition, give the engine output in terms of power, torque, and exhaust gas composition. Specific fluid dynamic models can be used to track the composition along the exhaust system and, with the aid of ad-hoc modules, to evaluate the conversion efficiency of after-treatment devices, such as TWC, GPF, DPF, DOC, SCR and so on.

This work is based on the idea of integrating two different 1D simulation tools in a co-simulation environment, realizing a strict coupling between the two codes. The main goal is to allow an accurate 1D simulation of the unsteady wave action and gas motion inside the intake and exhaust systems, without resorting to over-simplified geometrical discretization, and to rely on advanced combustion models for the calculation of cylinder-out emissions. The simulation of the after-treatment systems is then performed resorting to a steady state model with a detailed chemistry approach. In this scenario, the choice of the coupling strategy is a key issue, since an unsteady model must be coupled to a steady-state one. In particular, this last element may flatten the unsteady pattern of the flow, imposing unreal boundary conditions at the engine exhaust manifold and increasing the risk of misleading results. For this reason, the chemical and the fluid-dynamic behaviour have been decoupled, allowing the 1D solver to propagate pressure waves along the complete system, preserving all the characteristic lengths (acoustic and fluid dynamic). For every after-treatment device a specific steady-state 1D model is used to predict the chemical phenomena and the heat transfer process involved. The boundary conditions for the steady state solver are given by the 1D unsteady model, suitably averaged over the time. The steady-state solution is then sent back to the 1D unsteady solver and suitably over imposed: temperature of the substrate, friction coefficient and gas composition. This co-simulation environment is validated against a real engine configuration which was tested at EMPA labs. An SI, 4 cylinder, turbocharged, CNG engine is simulated at different loads and speeds and the results are compared with the experimental measurements, to verify the prediction of engine performance and pollutant emissions.

## 3 Methodology

### 3.1 Governing equations

The code used in this work is *gasdyn*, a 1D thermo-fluid dynamic model that is being continuously developed and enhanced by the researchers of Politecnico di Milano and Exothermia. The main features of the numerical code have been described in previous works [1-4]. The model has been developed for the simulation of internal combustion engines coupled to their intake and exhaust systems. This allows for a detailed analysis of the fluid dynamic, thermal and chemical behaviour of the whole engine system. The

differential equations describing the mass, momentum and energy conservation for each computational mesh are written in matrix form as follows [1-2]:

$$\frac{\partial \mathbf{W}(\mathbf{x}, t)}{\partial t} + \frac{\partial \mathbf{F}(\mathbf{W})}{\partial x} + \mathbf{B}(\mathbf{W}) + \mathbf{C}(\mathbf{W}) = 0$$

$$\mathbf{W} = \begin{bmatrix} \rho F \\ \rho U F \\ \rho e_0 F \end{bmatrix}, \quad \mathbf{F}(\mathbf{W}) = \begin{bmatrix} \rho U F \\ (\rho U^2 + p) F \\ \rho U h_0 F \end{bmatrix}, \quad \mathbf{B}(\mathbf{W}) = \begin{bmatrix} 0 \\ -p \frac{\partial F}{\partial x} \\ 0 \end{bmatrix}, \quad \mathbf{C}(\mathbf{W}) = \begin{bmatrix} 0 \\ \frac{2}{D} \rho U |U| f_w F \\ -\rho(q + q_{re}) F \end{bmatrix}$$

The source term  $q_{re}$  in the energy equation represents the heat released by the chemical reactions occurring in the gas phase (per unit mass per unit time) and  $q$  is the sum of the convective and radiative heat transferred from the gas to the pipe walls. The information concerning the tracking of chemical composition along the duct systems is accounted for by solving the mass conservation equation for each chemical specie considered:

$$\frac{\partial \rho Y_i F}{\partial t} + \frac{\partial (\rho Y_i U F)}{\partial x} = \dot{Y}_i$$

where  $Y_i = m_i/m$  is the mass fraction in the control volume for the  $i$ -th specie and  $\dot{Y}_i$  is the rate of variation of mass fraction due to chemical reactions involving the  $i$ -th specie. The system of conservation equations represents a quasi-linear hyperbolic problem which can be solved by means of shock-capturing numerical methods: the *gasdyn* code makes use of a set of different numerical solvers, among which symmetric, TVD finite difference techniques with 2nd order accuracy described in [5]. Boundary conditions and intra pipe connections for the representation of devices such as turbochargers, multipipe junctions, inlet and outlet and similar, are based on the method of characteristics [6,7].

For the purpose of this work the *gasdyn* code has been coupled to the *axisuite*® code, developed by Exothermia, which is able to deal with any reaction scheme and rate expressions (“elementary” and “global” reactions) [8,9,10].

### ***Balance equations***

The *axisuite* model adopted in this work exploits the assumption of simplified single channel. In this context the calculation of the temperature and species concentrations in the channel is based on the solution of the quasi-steady equations for the gas phase heat and mass transfer:

$$\rho_g C_{p,g} v_g \frac{\partial T_g}{\partial z} = -h \cdot \left( \frac{S_F}{\varepsilon} \right) \cdot (T_g - T_s)$$

where  $\rho$  is the density,  $C_p$  the specific heat capacity,  $v$  the gas velocity,  $T$  the temperature,  $h$  the heat transfer coefficient,  $S_F$  the monolith specific surface area and  $\varepsilon$  the

substrate void fraction. Subscripts  $g$  and  $s$  denote the exhaust gas and the solid substrate respectively.

Similarly, a “film” approach is also used to account for the gas phase mass transfer resistance:

$$\frac{\partial(v_g y_{g,j})}{\partial z} = -k_j \cdot \left(\frac{S_F}{\varepsilon}\right) \cdot (y_{g,j} - y_{s,j})$$

where  $y_j$  is the molar fraction of species  $j$  and  $k_j$  the mass transfer coefficient of species  $j$ . In these equations the heat and mass transfer coefficients are calculated based on the following definitions:

$$h = \frac{Nu \cdot \lambda_g}{d_h}, \quad k_j = \frac{Sh \cdot D_{mol,j}}{d_h}$$

where  $\lambda_g$  the thermal conductivity,  $D_{mol,j}$  the molecular diffusion and  $d_h$  the hydraulic diameter. Provided that the influence of internal diffusion is considered negligible, there is no concentration gradient in the washcoat and therefore only one surface species concentration is defined. Therefore, the total reaction rate on the surface for each species (including storage reactions) is equal to the local external species mass transfer to/from the exhaust gas:

$$\frac{\rho_g}{M_g} k_j \left(\frac{S}{\varepsilon}\right) (y_{g,j} - y_{s,j}) = R_j$$

where  $M_g$  is the gas molecular weight. The surface reaction rates for each species  $R_j$  are calculated based on the specific reaction scheme and are functions of local surface concentrations, coverages and temperature.

The thermal balance of solid phase is taken into account by solving the energy conservation equation also accounting for the transient behaviour:

$$\rho_s c_{p,s} \frac{\partial T_s}{\partial t} = \lambda_s \frac{\partial^2 T_s}{\partial z^2} + Sh \left(\frac{S}{1-\varepsilon}\right) (T_g - T_s) + \frac{1}{1-\varepsilon} \sum_{k=1}^{n_k} \Delta H_k R_k$$

which considers, in the right hand side, the contribution of convective heat transfer of the gas flow in channels and of the heat released or adsorbed by chemical reactions and adsorption.

In many catalyst applications, the thickness and effective diffusivity of the active layer may not allow the simplifying assumption of negligible internal diffusion resistance. In these cases, a more detailed approach which models mass transfer both in the gas phase and in the washcoat active volume pores may be used.

## 4 Coupling strategy

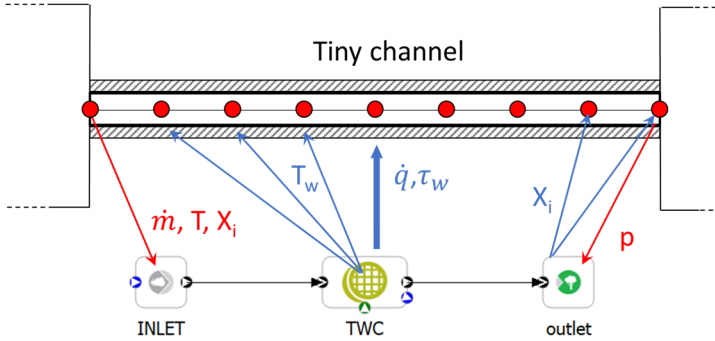


Figure 1. Schematic of the strategy adopted to couple *gasdyn* with *axisuite*.

To perform the simulation of the after-treatment system the *gasdyn* code has been coupled to *axisuite*. Since the numerical approaches of the two codes are different, the authors have developed a hybrid coupling to let an unsteady approach and a steady state one coexist in the same simulation framework. The main target of the developed strategy is two preserve the unsteady nature of the flow, with the transport of pressure pulsations, while exploiting the detailed calculation of the chemical reactions provided by the steady state solver. To achieve this goal the coupling approach is based on the duplication of the catalyst element, to generate two overlapping elements that are solved in parallel and suitably merged in the final solution. The fluid dynamics, meaning the wave action and the flow pulsations, is solved by *gasdyn* relying on the described numerical methods and on a characteristic-based approach [6] for the handling of intrapipe and domain boundary conditions. The passage of values from *gasdyn* to *axisuite* relies on the averaging of mass flow, gas temperature and chemical composition along a single, or a fraction, thermodynamic cycle. These averaged pipe quantities, as shown in Figure 1, are assigned as inlet boundary conditions to *axisuite*. In this framework, the time step used for the integration of the steady state problem is larger than the time step used in *gasdyn*, which is subject to the CFL stability condition. Therefore, during the *axisuite* time step, quantities are integrated at the inlet and then used to perform the steady state calculation, when the cumulative time step of *gasdyn* has reached the *axisuite* one. Once *axisuite* has performed its time step, the solution is then mapped back to *gasdyn*, transferring the quantities referred to the chemical activity and to the fluid dynamic processes occurring inside the catalyst: the wall temperature calculated node by node, the gas-wall heat flux at every node, the friction factor and the outlet species

concentrations. The heat flux and the friction factor are then considered in *gasdyn* as source terms in the governing equations ( $f_w$  and  $q$ ) and they are fully integrated in the stencil of the numerical method. The outlet concentration of chemical species is overwritten to the concentration tracked by *gasdyn*. This can be realized only with the option of constant thermo-physical properties implemented in the *gasdyn* solver: the  $c_p$  and molecular mass of the gas are considered constant regardless of the changes in the gas composition. The outlet concentration of *axisuite* is assigned to the last and second last node of the *gasdyn* domain and then passed as a zero-gradient trend to the characteristic-based approach. This will permit to advect along the path line the desired concentration and to track it downstream of the catalyst, following the pulsations of the gas flow.

## 5 Engine modelling

The first step of this research activity required a complete 1D modeling of the engine, on the basis of the known geometrical layout, including complex devices such as the NG injectors, the intercooler and the three-way catalysts. In Figure 2 the schematic of a SI, turbocharged, natural gas engine, realized by means the *gasdyn* graphical interface, has been depicted: all the geometrical characteristics of the intake and exhaust systems, including the turbocharger group with wastegate and the air cooler have been introduced. Figure 2 shows also the three catalysts placed along the exhaust line, which have been coupled with the *axisuite* code and the schematic of the representation of a single channel.

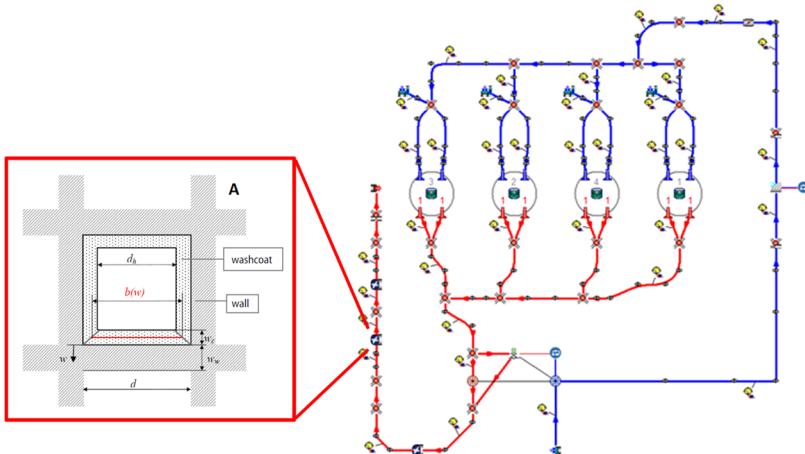


Figure 2. Schematic of the light duty 3.0L SI NG turbocharged engine realized by means the graphical interface *gasdynpre*.

The focus of this work was to investigate the behaviour of the after-treatment section, therefore only the first part of the exhaust system (without the silencers) was considered. The 1D model was applied in order to run a first level analysis, able to characterize the overall performance of the engine. As a second step, detailed simulations were carried out to confirm the validity of the *gasdyn-axisuite* coupling, in order to investigate the behaviour of the catalysts by a chemical point of view. The 1D modeling of the turbocharger represents a challenging task. The most common approach is based on the use of performance steady-flow maps [7], which are determined experimentally by the manufacturer and stored by the simulation model into dedicated look-up tables. About the SI combustion model, a primary requirement is an accurate prediction of the flame front velocity, which is influenced by a large number of factors, such as thermodynamic and chemical properties, turbulence intensity, chamber design and heat fluxes through the boundaries. In order to predict realistic values for the in-cylinder pressure traces, a multi-zone, quasi-dimensional combustion model has been used for the simulation of the spark ignited turbocharger engine, to evaluate the thermodynamic and chemical gas properties inside the combustion chamber [4] where the fully developed turbulent flame speed has been computed applying the Zimont model [11]. Therefore, even accepting all limitations due to a quasi-dimensional approach, it is fundamental to account for the turbulence generation and dissipation within the combustion chamber and to rely on appropriate laminar flame speed correlations. For the former aspects, the turbulent intensity  $u'$  has been evaluated by the two-equation model k-K from the knowledge of the turbulent kinetic energy,  $k$ , and the mean flow kinetic energy,  $K$  [4]. The convective heat transfer rate to the combustion chamber walls is calculated as indicated in [4], whereas the heat transfer coefficient has been calculated by applying the Woschni correlation [12].

## 5.1 Engine type

In this study a light duty 3.0L SI, NG, turbocharged engine was considered. The engine is fuelled by natural gas (NG), which is injected inside the primary ducts by a port fuel injection (PFI) system, adopting a sequential and phased strategy. The engine is supercharged by means of a turbocharging group with a single stage fixed geometry (FG) turbine and a wastegate (WG). In the induction system an intercooler is adopted, in order to increase the volumetric efficiency and to reduce the knocking propensity. Three catalysts are located downstream of the turbine: one pre-cat, based on a metallic support, one ceramic main catalyst and a third monolith, not loaded with precious metals. This engine has been instrumented and investigated experimentally on the test bench at EMPA labs, to study and optimize the combustion process and reduce the pollutant emission formation. The main specifications of the engine investigated are reported in Table 1.

## 5.2 Discussion of results

The initial step has been an extended validation of the 1D simulation on the basis of experimental measurements. These simulations have been carried out for some operating points at full load, from minimum up to maximum engine speed, as well as at part load at 2000 rpm.

Table 1. Main specification of the light duty 3.0L SI NG turbocharged engine.

<b>Engine</b>	4 stroke, 4 valves per cylinder
<b>ic capacity [dm<sup>3</sup>]</b>	3.0
<b>Supercharging</b>	single stage FG turbo-
<b>Cylinder arrangement</b>	Four in line
<b>Cylinder bore [mm]</b>	95.8
<b>Fuel supplier</b>	PFI
<b>Fuel</b>	Natural Gas

With regard to the simulations at full load, the comparisons between measured data and predicted results are useful to evaluate the correct behaviour of the turbocharger group and to analyse the values of the main fluid-dynamic parameters (air mass flow, gas pressure and temperature along the duct systems, etc.).

Figures 3 and 4 show the comparison between experiments and prediction of air mass flow rate delivered by the compressor, as well as the boost pressure achieved, the latter being targeted by a PID controller. The good agreement between the measured and computed data is also due to the well captured interaction between the gas injected into the primary ducts and the mass flow towards the cylinders. As expected, the natural gas injection points out a significant influence on the air mass flow rate, due to its high specific volume, which limits the air mass into the cylinder during the induction phase.

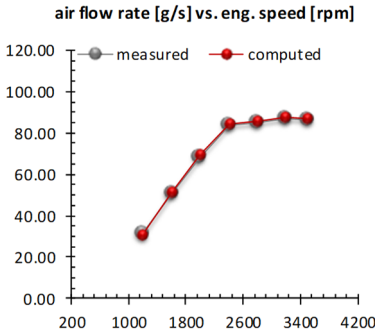


Figure 3. Air mass flow rate [g/s] plotted as a function of engine speed [rpm]. Full load conditions.

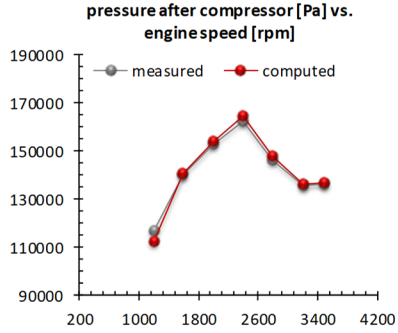


Figure 4. Boost pressure [Pa] downstream of the compressor, plotted as a function of engine speed [rpm]. Full load conditions.

In Figure 5, for the sake of completeness it is reported the comparison between the computed and the measured air temperature after the compressor. This, once again, points out that the map-based model of the turbocharger unit is reliable in predicting the fluid dynamic processes occurring inside the turbine and the compressor. Downstream of the compressor, the intercooler performs the cooling of the fresh charge reaching the delivery gas temperature thanks to the PID controller set on the gas temperature.

In the model, the fuel mass is injected according to the experimental injection strategy fixed by ECU (in terms of mass injected per cycle and timing). In this way the corresponding in-cylinder air-fuel ratio is determined only by the local thermo-fluid dynamic conditions into the ducts and by the possible differences among the volumetric efficiency for each cylinder.

In order to predict realistic values of in-cylinder pressure traces, a multi-zone, quasi-dimensional combustion model [4] has been applied for the simulation of the engine, to evaluate the thermodynamic and chemical gas properties into the combustion chamber. The correct flame front velocity propagation depends on the turbulence intensity in the cylinder and on the A/F ratio, which define the laminar flame speed, the turbulent flame speed and, as a consequence, the correct heat release ratio. In particular, the model uses the actual spark timing (data extracted from the ECU). In Figure 6 the calculated in-cylinder peak pressure is compared with the corresponding measured value.

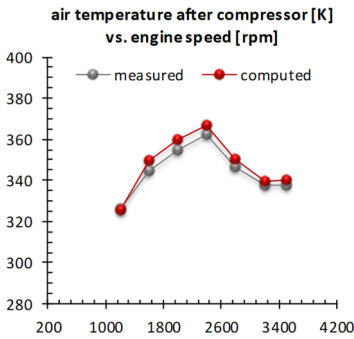


Figure 5. Air temperature [K] inside the duct after compressor, plotted as a function of engine speed [rpm]. Full load conditions.

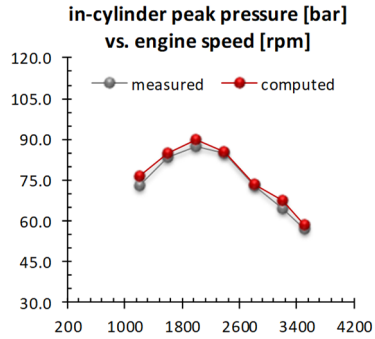


Figure 6. In-cylinder peak pressure [-], plotted as a function of engine speed [rpm]. Full load conditions.

Once the global parameters have resulted in rather good agreement with the experimental data, the 1D model can be used also to predict the cylinder-out pollutant emissions, in order to transport the chemical species along the exhaust ducts and then evaluate the conversion process through the catalysis. The *gasdyn* code is able to predict the concentration of the main species such as  $\text{NO}_x$ , CO,  $\text{CO}_2$ , HC,  $\text{O}_2$ , etc, during the combustion process and their concentration in the exhaust gases discharged by cylinders at EVO.

The calculation procedure of the chemical composition of the exhaust gas in the cylinder, implemented in the *gasdyn* code, is based on the method described in [13] to evaluate the equilibrium concentrations of the major species. In addition, the extended 6 reaction Zeldovich model was used to simulate the kinetically controlled  $\text{NO}_x$  formation process. This assumption relies on the fact that the oxygen consumed by the NO formation is negligible with respect to the oxygen reacting during the combustion, so that the corresponding heat of reaction can be neglected in the calculation of the gas temperature [14,15].

The CO concentration has been computed by applying the Baruah semi-empirical method on the basis of the maximum equilibrium values achieved in the combustion chamber [4]. However, such a method is not fully predictive, since it must be calibrated at least for one operating point. Separate models describe the unburnt hydrocarbons formation, considering individually the contribution due to the crevices, the oil film layer and the partial burn in the chamber [4].

Figure 7 shows the normalized  $\text{NO}_x$ , CO, HC and  $\text{O}_2$  concentrations discharged by the cylinders at EVO. It is possible to notice that the trend is in rather good agreement with the measured data. In particular the  $\text{NO}_x$  trend changes, as a function of engine speed,

according to the A/F ratio and the in-cylinder peak pressure. With regard to CO and HC concentrations (the latter expressed as carbon equivalent), the emission sub-models have been tuned at 1200 rpm, full load, and the same tuning values have been used for all the operating conditions. The tuning of HC has also an influence on the computed O<sub>2</sub> concentration mainly because of its presence in the mixture stored and released by the crevices and this explain why the proposed tuning for the HC submodels does not match the experimental value for any operating condition.

Concerning the simulations at variable load and constant regime, the comparison between computed and measured data is related to six different loads, identified as percentage of the maximum BMEP at 2000 rpm. In particular, the load percentages are the following: 25%, 35%, 45%, 55%, 65% and 75%.

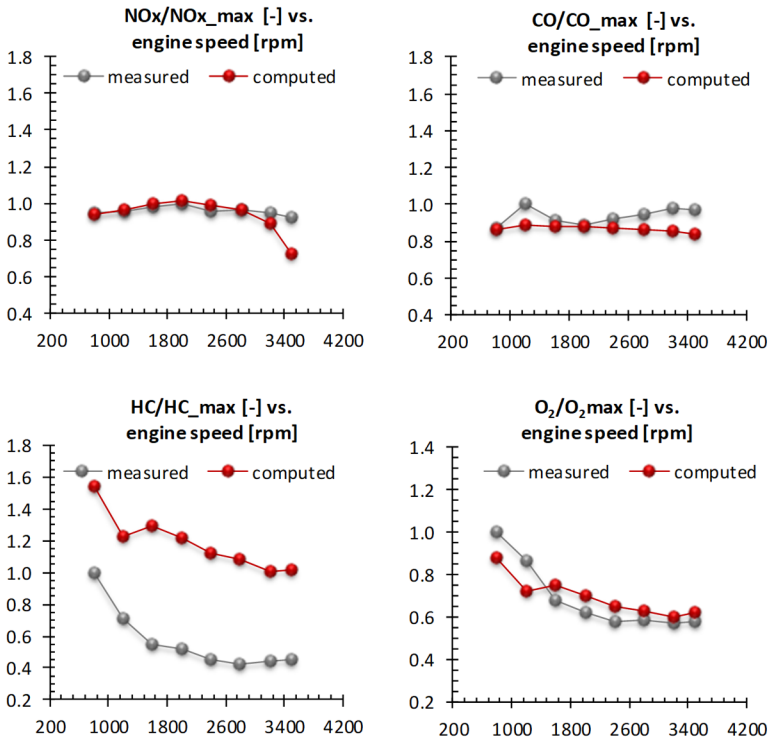


Figure 7. Main pollutant emissions (concentration normalized over the maximum value) discharged by the cylinders. Comparison between measured and computed data, full load operating conditions.

In Figure 8 some typical global parameters have been reported. In particular, the computed turbocharger speed, the air mass flow rate, the BMEP and the in-cylinder peak pressure have been compared to the measured data. As can be noted, it shows a rather good agreement between the two sets of data, pointing out the reliable prediction of the model also at partial loads.

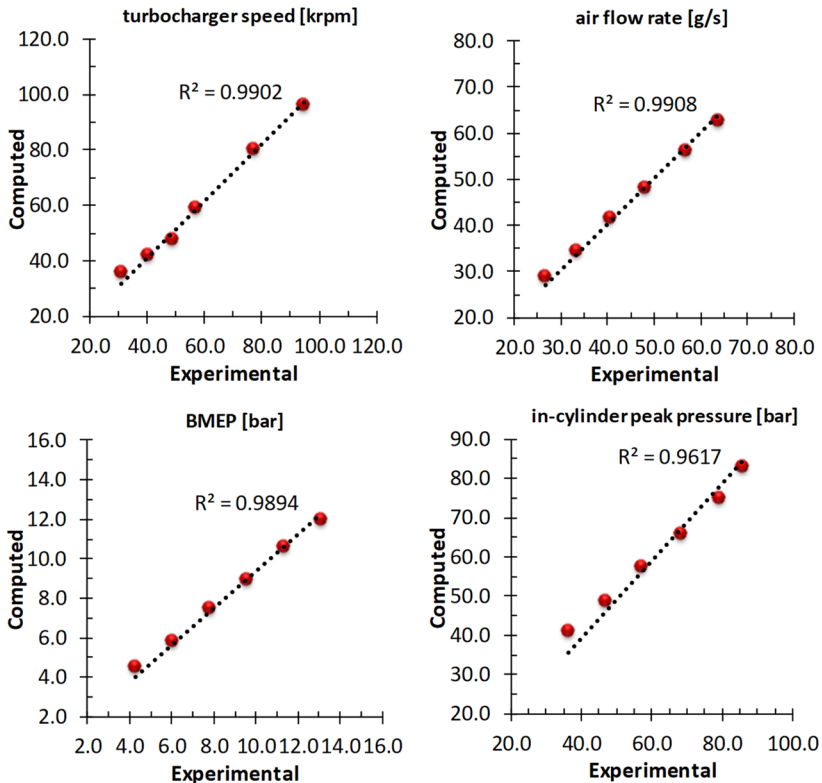


Figure 8. Experimental and calculated turbocharger speed, air mass flow rate, BMEP and in-cylinder peak pressure for the six operating points at partial loads ((as percentage of the maximum BMEP: 25%, 35%, 45%, 55%, 65% and 75%).

For the same operating points at part load reported in Figure 8, the corresponding cylinder-out emissions have been computed and compared to the experimental data. Figure 9 shows the normalized CO, CO<sub>2</sub>, HC and O<sub>2</sub> concentrations discharged by the cylinders at EVO.

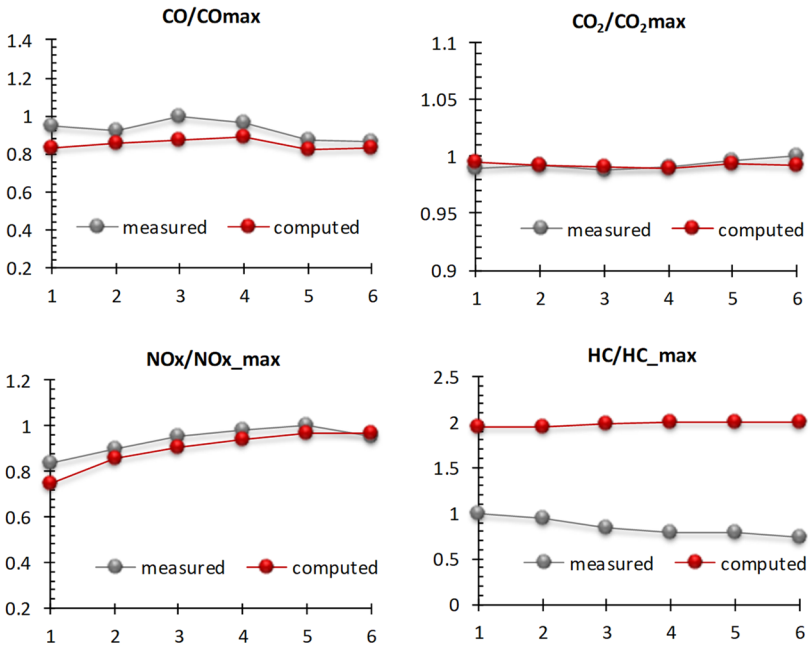


Figure 9. Experimental and calculated CO, CO<sub>2</sub>, NO<sub>x</sub>, HC emission concentration (normalized over the maximum value) for the six operating points at partial load (as percentage of the maximum BMEP: 1=25%, 2=35%, 3=45%, 4=55%, 5=65% and 6=75%).

The cylinder-out gas composition calculated by *gasdyn* is then tracked downstream of the cylinder head, along the exhaust system, thanks to the possibility of advecting the information about the chemical composition of the gas. Along the exhaust line the gas stream flows through the catalyst converter where, by means of the coupling with *axisuite*, the heterogeneous reactions occurring on the washcoat surface are modeled.

Figure 10 shows the comparison between the measured and calculated species conversion of CH<sub>4</sub>, CO, NO<sub>x</sub> and O<sub>2</sub> across the whole after-treatment system (ATS): precat and main catalyst. From the analysis of the combustion process in the previous section, it appears that the exhaust gas contains both oxygen and unburned hydrocarbons due to the particularly slow kinetics of CH<sub>4</sub> at cylinder level. This results in a gas composition typical of lean burn conditions where O<sub>2</sub> is present, even if the engine feeding condition were slightly rich.

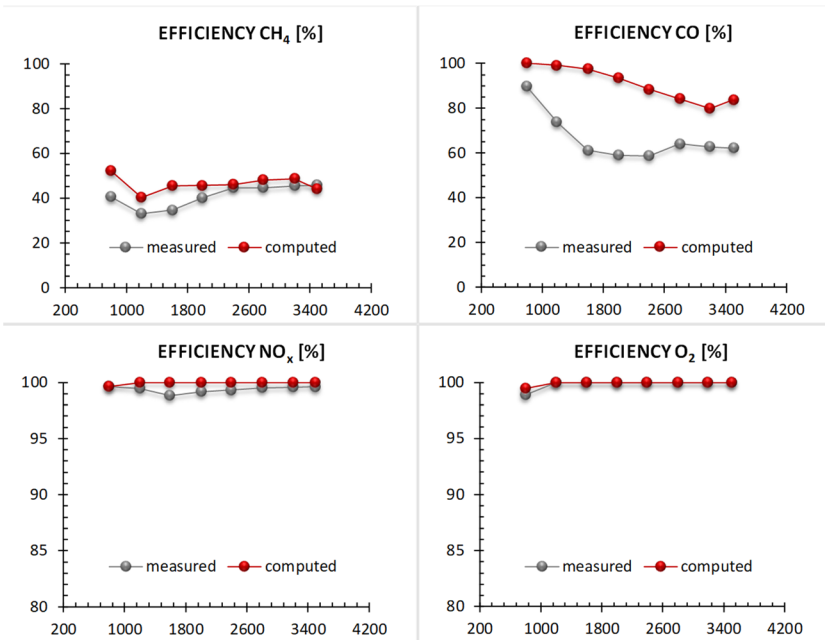


Figure 10. Experimental and calculated CH<sub>4</sub>, CO, NO<sub>x</sub> and O<sub>2</sub> conversion across the ATS: full load condition.

The catalysts equipped on this exhaust system are typical TWC for SI engines. Despite the geometrical parameters of the three catalysts where fully known, the chemical composition of their washcoats, was guessed on the basis of typical catalyst properties, since the manufacturer have not provided complete information about them. Therefore, these devices have been modelled exploiting the predefined chemical libraries of *axisuite* for the simulation of three way catalysts. As can be seen in Figure 10, the oxygen contained in the gas stream is consumed completely in every operating condition. This is due to the presence of CO, ceria oxides (at washcoat level) and to the presence of CH<sub>4</sub>, which are competing towards the oxygen. These oxidation reactions appear to be important in the first part of the ATS. Then, in the second part, thanks to the complete conversion of O<sub>2</sub>, the suitable environment in the exhaust gas to reduce NO<sub>x</sub> consuming CO has been created. The comparison with the measured data shows that the calculations can predict the conversion of CH<sub>4</sub> and NO<sub>x</sub>, whereas the conversion of CO suffers the lack of information about the washcoat composition.

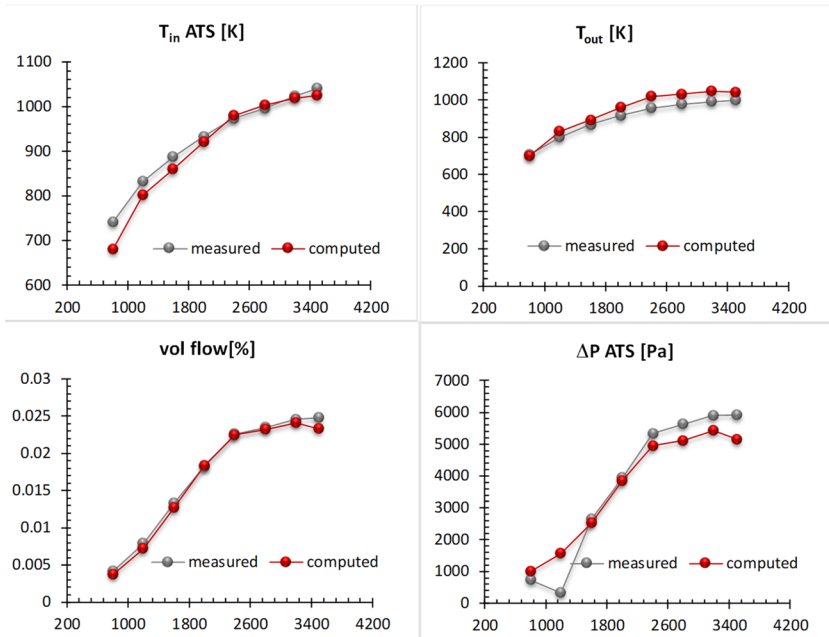


Figure 11: Comparison between experimental and calculated quantities: gas temperature at the inlet of the precat ( $T_{in}$ ), gas temperature at the outlet of the main catalyst ( $T_{out}$ ), volumetric flow ant the inlet of the ATS and pressure drop across the ATS.

Figure 11 shows the comparison between the calculated and the measured fluid dynamic quantities. In particular, the gas temperature at the inlet of the ATS is presented, showing that the model can predict correctly the heat transfer in the pre turbine exhaust manifold and also the expansion of the gas through the turbine. A correct prediction of the gas temperature at the inlet is important to evaluate the volumetric flow at the inlet of the ATS and therefore the pressure loss caused by the resistance of the substrate. Moreover, the comparison between the measured and calculates gas temperature, shoe that there is an overestimation of the temperature level. This, since this temperature reflect the chemical activity of the catalysts, can be explained by the overestimation of the CO oxidation reaction.

## 6 Conclusions

In this paper the application of an integrated approach based onto a strict coupling between the *gasdyn* and *axisuite* code has been proposed with the main goal of allowing the detailed simulation of engine performance based on unsteady 1D models with detailed modelling of chemical reactions in the after-treatment devices. To this purpose the authors have developed an original strategy to couple a code based on the unsteady formulation of the conservation equations, necessary to capture the wave action in the ducts and to estimate the engine performance, to a steady state approach for the simulation of after treatment systems. The strategy makes possible the continuous passage of information between the codes at synced time steps, due to the difference of the time marching procedure of the codes. The developed approach has been tested on an industrial case: 4 cylinder, spark ignition, CNG fuelled, heavy duty engine. Several operating conditions at partial and at full load condition, for different engine revolution speeds, have been simulated, showing that the global engine performance parameters can be predicted with fairly good accuracy as well as engine out emissions. The coupling strategy has proved to be successful in allowing the flow unsteadiness to propagate along the system, while advecting the chemical composition from the engine head to the tail pipe through the catalytic devices. The simulation results have shown that by the coupling it is possible to predict the abatement of chemical components such as CH<sub>4</sub>, NO<sub>x</sub> and CO inside converters placed in cascade configuration. The agreement with the measured abatement efficiency has shown that, globally, the matching is encouraging, with the exception of the CO caused by the lack of information about the composition of the washcoats of the catalysts.

## Bibliography

1. Montenegro, G., Onorati, A., Della Torre, A., The prediction of silencer acoustical performances by 1D, 1D-3D and quasi-3D non-linear approaches. *Computers and Fluids*, 71, pp. 208-223, 2013.
2. Cornolti, L., Onorati, A., Cerri, T., Montenegro, G., Piscaglia, F., 1D simulation of a turbocharged Diesel engine with comparison of short and long EGR route solutions. *Applied Energy*, 111, pp. 1-15, 2013.
3. Stockar, S., Canova, M., Guezennec, Y., Torre, A.D., Montenegro, G., Onorati, A., Modeling wave action effects in internal combustion engine air path systems: Comparison of numerical and system dynamics approaches. *International Journal of Engine Research*, 14 (4), pp. 391-408, 2013.
4. D'Errico G., Ferrari G., Onorati A., Cerri T., Modeling the Pollutant Emissions from a S.I. Engine, SAE paper n. 2002-01-0006, 2002.

5. Corberan, J.M., Gascon, M.L., Construction of Second Order TVD Schemes for Non-Homogeneous Hyperbolic Conservation Laws. *Journal of Computational Physics*, vol. 172, 261-297, 2001.
6. D. E. Winterbone and R. J. Pearson. *Theory of engine manifold design*. Professional Engineering Publishing, London, 2000
7. Serrano J.R., Arnau F.J., Dolz V., Tiscira A., Cervelló C., A model of turbocharger radial turbines appropriate to be used in zero- and one-dimensional gas dynamics codes for internal combustion engines modeling. *Energy Convers Manage* 2008; 49(12): 3729-45.
8. Tsinoglou D. and G. Koltsakis, "Modelling of the selective catalytic NOx reduction in diesel exhaust including ammonia storage", *Proceedings of the Institution of Mechanical Engineers, Part D: Journal of Automobile Engineering*, 221(1): 117-133, 2007
9. Koltsakis, G.C., P.A. Konstantinidis and A.M. Stamatelos, "Development and application range of mathematical models for 3-way catalytic converters", *Applied Catalysis B: Environmental*, 12(2-3): 161-191, 1997
10. Tsinoglou, D.N., G.C. Koltsakis and J.C. Peyton Jones, "Oxygen Storage Modeling in Three-Way Catalytic Converters", *Industrial & Engineering Chemistry Research*, 41(5): 1152-1165, 2002
11. Lipatnikov A.N., Choimiak J., Turbulent flame speed thickness: phenomenology, evaluation, and application in multi-dimensional simulations. *Prog. Energy Combustion* 2002; 28:1-73.
12. Heywood J.B., *Internal Combustion Engine Fundamentals*. Mc Graw Hill, 1998
13. Erickson W.D., Probhhu R.K., Rapid Computation of Equilibrium Composition: an Application to Hydrocarbon Combustion. *A.I.Ch.E. Journal*, vol. 32 no. 7, July 1986.
14. Lavoie G., Blumberg P.N., A fundamental Model for Predicting Fuel Consumption, NOx, and HC Emissions of the Conventional Spark-Ignition Engines, *Combustion Science and Technology*, Vol. 21, pp 225-258, 1980.
15. Lavoie G., Adamczyk A.A., Kaiser E.W., Cooper J.W., Rothschild W.G. R, *Engine HC Emissions Modeling: Partial Burn Effects*, *Combustion Science and Technology*, Vol. 9, pp 99-105, 1986.